Gene-trapped mouse embryonic stem cell-derived cardiac myocytes and human genetics implicate *AKAP10* in heart rhythm regulation

Whittemore G. Tingley*[†‡], Ludmila Pawlikowska[§], Jonathan G. Zaroff[†], Taeryn Kim*, Trieu Nguyen*, Stephen G. Young[¶], Karen Vranizan*[‖], Pui-Yan Kwok[§], Mary A. Whooley[†**], and Bruce R. Conklin*[†,††‡‡]

*Gladstone Institute of Cardiovascular Disease, San Francisco, CA 94158; [§]Cardiovascular Research Institute and Departments of [†]Medicine and [††]Cellular and Molecular Pharmacology, University of California, San Francisco, CA 94143; [¶]Department of Medicine, University of California, Los Angeles, CA 90095; [‖]Functional Genomics Laboratory, University of California, Berkeley, CA 94720; and **Veterans Affairs Medical Center, San Francisco, CA 94143

Edited by Susan S. Taylor, University of California at San Diego, La Jolla, CA, and approved March 29, 2007 (received for review November 28, 2006)

Sudden cardiac death due to abnormal heart rhythm kills 400,000–460,000 Americans each year. To identify genes that regulate heart rhythm, we are developing a screen that uses mouse embryonic stem cells (mESCs) with gene disruptions that can be differentiated into cardiac cells for phenotyping. Here, we show that the heterozygous disruption of the *Akap10* (D-AKAP2) gene that disrupts the final 51 aa increases the contractile response of cultured cardiac cells to cholinergic signals. In both heterozygous and homozygous mutant mice derived from these mESCs, the same *Akap10* disruption increases the cardiac response to cholinergic signals, suggesting a dominant interfering effect of the *Akap10* mutant allele. The mutant mice have cardiac arrhythmias and die prematurely. We also found that a common variant of *AKAP10* in humans (646V, 40% of alleles) was associated with increased basal heart rate and decreased heart rate variability (markers of low cholinergic/vagus nerve sensitivity). These markers predict an increased risk of sudden cardiac death. Although the molecular mechanism remains unknown, our findings in mutant mESCs, mice, and a common human *AKAP10* SNP all suggest a role for AKAP10 in heart rhythm control. Our stem cell-based screen may provide a means of identifying other genes that control heart rhythm.

G protein | receptor | signaling

In mammalian species, basal heart rate (HR) correlates inversely with lifespan. Among healthy humans, basal HR correlates inversely with overall survival and correlates directly with the risk of sudden cardiac death (1). HR is regulated by neural and hormonal signals that compete to stimulate or inhibit the cardiac pacemaker. Adrenergic signals activate β-adrenergic receptors (βARs) in pacemaker cells to increase cAMP concentration, activate protein kinase A (PKA), and increase pacemaker rate. In contrast, cholinergic signals activate M2 cholinergic receptors (mAChRs) to decrease cAMP levels and slow pacemaker rate. People with lower vagus nerve/cholinergic sensitivity have faster basal HR, less variability of HR (HRV), and higher risk for sudden cardiac death (2). Inhibition of adrenergic signals with βAR antagonists improves survival in patients suffering common cardiac diseases.

cAMP and PKA regulate numerous proteins throughout cardiac cells to control many cardiac functions in addition to heart rate. The subcellular distribution, timing, and downstream effects of cAMP and PKA activity are coordinated in large part by a family of intracellular scaffolding proteins called A-kinase-anchoring proteins (Akaps). Akaps bind and localize PKA within protein complexes that can include receptors (3–5), enzymes that produce and degrade cAMP, other cell-signaling proteins, and downstream PKA substrates and effector proteins (3, 6, 7). Variations in the genes that regulate cAMP and PKA signaling may determine individual susceptibility to abnormal heart rhythms and responses to cardiac medications (8).

To attempt to determine which proteins coordinate the effects of cAMP and PKA on cardiac rhythm, we combined a cell-culture model of the cardiac pacemaker with an efficient method for gene inactivation. Mouse embryonic stem cells (mESCs) in culture readily differentiate into cardiac myocytes that contract spontaneously and closely resemble cardiac pacemaker cells (9, 10). mESCs are amenable to a variety of gene inactivation approaches, including high-throughput gene trapping. Gene-trapping efforts have disrupted >40% of mouse genes in mESCs (www.GeneTrap.org), providing a large and growing resource to test gene function. Here, we describe the cardiac rhythm disturbances caused by gene-trap disruption of *Akap10*.

Evolutionary conservation of *AKAP10*, including the PKA binding domain [Fig. 1 and supporting information (SI) Fig. 4], suggests that *AKAP10* serves a critical function in diverse species (11). The human gene is polymorphic in the PKA-binding domain at position 646, resulting in protein isoforms with different affinities for PKA that correlate with different cellular localizations (11–13). The predominant isoform, 646I, has a lower affinity for PKA than the minor isoform 646V. Interestingly, the 15 available nonhuman vertebrate *AKAP10* gene sequences, including chimp, all encode valine at position 646, suggesting that 646I is unique to humans. 646I constitutes ≈60% of Caucasian and Hispanic human alleles and is more common in Asian Americans (≈80%), but is the minor allele in African Americans (≈40%) (refs. 11 and 15 and W. Tingley, J. Zaroff, and M. Whooley, unpublished data from the Heart and Soul Study).

Results

***Akap10* Mutation Alters Cardiac Response to Cholinergic Agonists in Cell Culture.** A recent, large-scale SNP association study suggested that the I646V SNP might affect cardiac electrical function and human health (11). To determine whether *Akap10* regulates heart rhythm in mice, we examined the effects of a mutation in mouse

Author contributions: W.G.T. and B.R.C. designed research; W.G.T., T.K., and T.N. performed research; W.G.T., L.P., J.G.Z., T.N., K.V., P.-Y.K., M.A.W., and B.R.C. contributed new reagents/analytic tools; W.G.T., L.P., J.G.Z., T.K., T.N., S.G.Y., K.V., P.-Y.K., M.A.W., and B.R.C. analyzed data; and W.G.T., S.G.Y., K.V., and B.R.C. wrote the paper.

The authors declare no conflict of interest.

This article is a PNAS Direct Submission.

Freely available online through the PNAS open access option.

Abbreviations: Akaps, A-kinase-anchoring proteins; AV, atrioventricular; βAR, β-adrenergic receptor; GIRK, G_i protein-gated inwardly rectifying potassium; HR, heart rate; PKA, protein kinase A; mAChR, M2 cholinergic receptor; mESC, mouse embryonic stem cell; RGS, regulator of G protein signaling.

[‡]Present address: CardioDx, 3183 Porter Drive, Palo Alto, CA 94304.

[‡‡]To whom correspondence should be addressed at: Gladstone Institute of Cardiovascular Disease, 1650 Owens Street, San Francisco, CA 94158. E-mail: bconklin@gladstone.ucsf.edu.

This article contains supporting information online at www.pnas.org/cgi/content/full/0610393104/DC1.

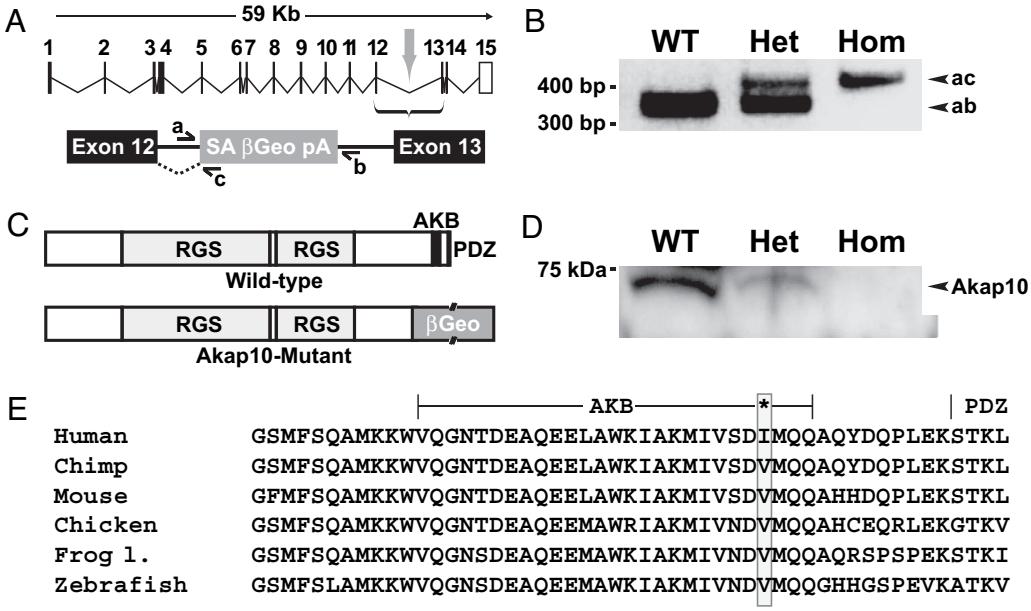

Fig. 1. Mutation of mouse *Akap10*. (*A*) Location of the gene-trap insertional mutation between exons 12 and 13 in *Ak10*. The inserted sequence (gray box) includes a splice acceptor (SA), selectable marker (''βGeo,'' a fusion of β galactosidase and neomycin phosphotransferase II), followed by a stop codon and a polyadenylation signal (pA). The insertion disrupts mRNA splicing and eliminates exons 13–15. (*B*) PCR products obtained by using primers (a, b, and c as indicated in *A*) and genomic DNA from WT, heterozygous (Het), and homozygous (Hom) *Akap10*-mutant mice. (*C*) Expected domain structures of WT and Akap10-mutant proteins. RGS, domains with homology to regulators of G protein signaling; AKB, PKA-binding domain; PDZ, PDZ-binding motif. (*D*) Immunoblots of cardiac Akap10 protein using an antibody generated against the 27-residue AKB domain. (*E*) Species alignment of the final 51 aa that are absent from Akap10-mutant protein. Asterisk indicates the human polymorphic I646V position. A full alignment for 16 species is shown in SI Fig. 4.

Akap10 on cardiac cells in culture. The *Akap10* mutation, which was generated in mESCs as part of our gene-trapping effort (16), truncates the protein C terminus and eliminates the last 51 aa that include its PKA-binding domain (Fig. 1). To derive *Akap10*-mutant cardiac cells, we induced the differentiation of *Akap10*-mutant mESCs in culture (10). The mutant mESCs differentiated into spontaneously contracting cardiac myocytes that were morphologically indistinguishable from cardiac myocytes derived from WT mESCs (SI Movie 1). However, the mutant myocytes contracted at a slightly slower rate than WT cells (25.3 ± 1.0 vs. 29.9 ± 1.2 contractions per minute, $P \leq 0.006$, $n = 114$ and 115), potentially indicating altered pacemaker function.

The slower contraction rate of the mutant cells suggested to us that Akap10 might contribute to the cholinergic/vagus nerve signaling pathway, which slows HR and increases HR variability. To determine whether the *Akap10*-mutant cells were more sensitive to cholinergic signals, we treated the cells with the cholinergic agonist carbachol. *Akap10*-mutant cells responded more to cholinergic agonist than WT cells (Table 1 and Fig. 2 *A* and *B*). The effect of the *Akap10* mutation was specific to cholinergic signaling, because an adrenergic agonist increased the contraction rate of WT and mutant myocytes to a similar degree (Table 1). We also noted that *Akap10*-mutant cells tended to have more variability in beat-to-beat intervals (analogous to HRV) and had significantly more variability after addition of cholinergic agonist (Table 2 and Fig. 2*A*). These findings indicate that the *Akap10* mutation facilitates cholinergic signaling in cultured cardiac cells, resulting in more HR slowing and more beat-to-beat variability.

***Akap10* Regulates Cholinergic and Vagus Nerve Sensitivity in Mice.** To determine whether Akap10 plays a similar role *in vivo*, we gener-

Table 1. Effects of the *AKAP10* mutation on HR regulation

		Rate, beats per min ± SE		
	Agonist drug type, *n*	Baseline	Treated	Fold change
Myocytes	mAChR cholinergic			
WT	66	28 ± 1	24 ± 1	0.84 ± 0.04
Akap10-mutant	66	26 ± 1	15 ± 2*	0.53 ± 0.05*
	β-adrenergic			
WT	31	30 ± 3	54 ± 4	1.91 ± 0.14
Akap10-mutant	32	22 ± 2¶	40 ± 3¶	2.05 ± 0.17
Mice	mAChR cholinergic			
Saline	9	630 ± 25	710 ± 20†	1.14 ± 0.04¶
WT	15	610 ± 20	600 ± 15	1.00 ± 0.04
Akap10-mutant	30	600 ± 15	490 ± 20*	0.83 ± 0.04‡
	α-adrengeric			
WT	12	620 ± 23	530 ± 22	0.87 ± 0.03
Akap10-mutant	24	590 ± 18	450 ± 19¶	0.77 ± 0.04

*, $P < 0.0001$; †, $P < 0.0005$; ‡, $P < 0.001$; §, $P < 0.01$; ¶, $P < 0.05$ (all vs. WT).

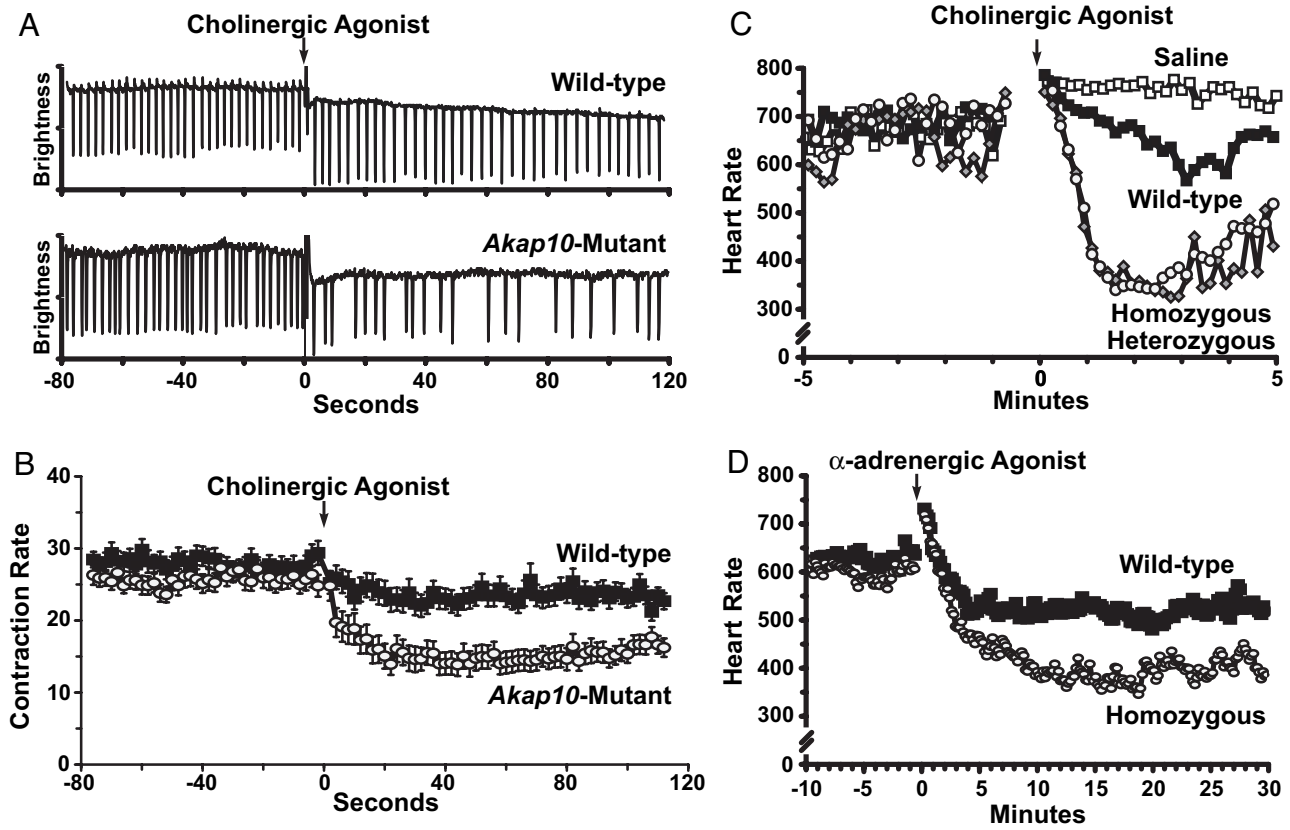

Fig. 2. Effects of the *Akap10* mutation on cholinergic/vagus nerve signaling *in vitro* and *in vivo*. (*A* and *B*) Response of mESC-derived cardiac myocytes to the cholinergic agonist carbachol. (*A*) Contractions (indicated by downward deflections in brightness) of representative WT and *Akap10*-mutant myocyte clusters before and after addition of the mAChR cholinergic agonist, carbachol (1 μM). Contractions were detected by phase microscopy as changes in light transmission during cell contraction. (*B*) Contraction rates of WT and *Akap10*-mutant myocytes before and after the mAChR cholinergic agonist. Data are mean (±SEM) for 66 WT and 66 *Akpa10*-mutant myocyte clusters. (*C* and *D*) HR regulation in *Akap10*-mutant mice. (*C*) A representative experiment showing HRs from WT (black squares), heterozygous (diamonds), and homozygous (circles) littermate mice before and after low-dose mAChR cholinergic agonist, methacholine (agonist better suited for mice) injection (2 mg/kg i.p.). The control mouse (white squares) was injected with saline vehicle. (*D*) Vagus nerve sensitivity in homozygous *Akap10*-mutant mice ($n = 12$) and WT littermates ($n = 12$) measured by the baroreflex. Baroreceptors in the carotid body sense hypertension induced by the arterial vasoconstrictor, and α-adrenergic agonist, phenylephrine (2 mg/kg i.p.) and stimulate the vagus nerve to slow HR. Values are means from three replicate experiments with four homozygous mutant and four WT mice.

ated mice from the same *Akap10*-mutant mESCs. Heterozygous and homozygous mutant mice were viable and had no abnormal developmental phenotypes. As with mESC-derived myocytes, treatment with cholinergic agonists caused more HR slowing in *Akap10*-mutant mice than in WT littermates (Table 1, Fig. 2*C*, and SI Fig. 5*A*). To indirectly assess endogenous cholinergic signals from the vagus nerve, we activated the vagus nerve by means of a baroreflex with the α-adrenergic receptor agonist phenylephrine. Compared with WT littermates, *Akap10*-mutant mice had stronger baroreflexes (more HR slowing), indicating higher vagus nerve sensitivity (Table 1 and Fig. 1*D*). These results suggest that the *Akap10* mutation increases the sensitivity of pacemaker cells to cholinergic inputs *in vivo*, as in culture.

Table 2. Effects of the *Akap10* mutation on beat-to-beat HR variability in cultured myocytes and conscious mice

		RMSSD (mean ± SE)	
	n	Baseline	mAChR agonist
Myocytes			
WT	66	720 ± 120	1,980 ± 790
Akap10-mutant	66	1,520 ± 450*	10,190 ± 2,360†
Mice			
WT	4	2.10 ± 0.32	NA
Homozygous	4	7.55 ± 1.71‡	NA

*, $P = 0.075$; †, $P < 0.0005$; ‡, $P < 0.05$; (all vs. WT). NA, not applicable.

To identify arrhythmias that might result from abnormally high vagus nerve sensitivity, we obtained continuous electrocardiograms (ECGs) from *Akap10*-mutant mice. Because stress inhibits vagus nerve activity, all recordings were obtained from undisturbed mice in their home cages. Homozygous mutant mice exhibited pronounced sinus arrhythmia (SI Fig. 5*B*) and abnormally high beat-to-beat HRV (Table 2 and Fig. 2*C*). The mechanism by which vagus nerve inputs increase beat-to-beat variability in mice is by activating G_i protein-gated inwardly rectifying potassium (GIRK, I_{KACh}) channels (17), which open upon binding the β- and γ-subunits of activated G_i. Therefore, our findings suggest that Akap10 inhibits this signaling pathway through a direct or indirect mechanism. Interestingly, Akap10 contains two domains with homology to "regulator of G protein signaling" (RGS) proteins (13, 18) (SI Fig. 4*C*), which could alter G protein signaling (19–25). Because the *Akap10* mutant has a dominant effect physiologically, the mutant allele may be interfering with the WT allele. Although we do not know the molecular mechanism of this interference, the *Akap10* mutant could provide a valuable tool to dissect this signaling pathway, just as dominant-negative alleles have been valuable for dissecting other pathways (e.g., N17R*as*) (26).

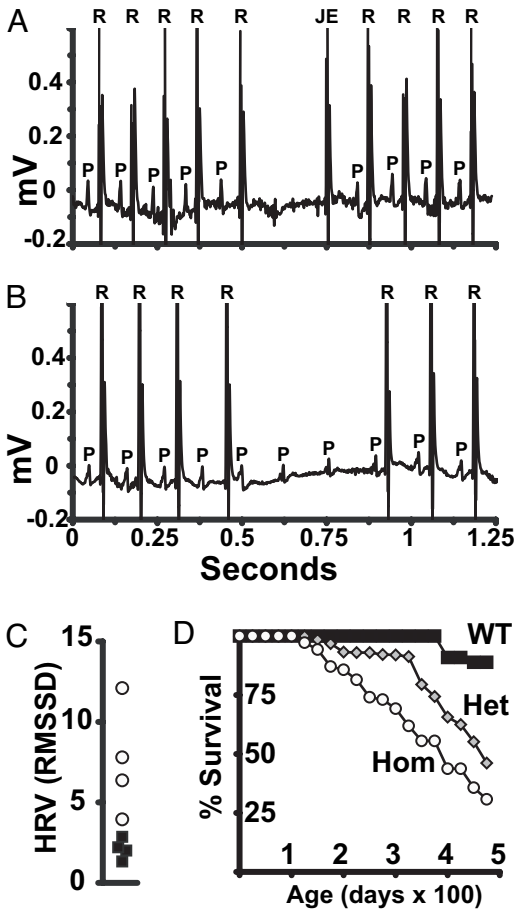

Fig. 3. Effects of *Akap10* on heart rhythm and survival in mice. (*A* and *B*) Spontaneous bradyarrhythmias in homozygous *Akap10*-mutant mice. ECG recordings demonstrating a sinus pause with a junctional escape (*A*) and AV block (loss of R waves) (*B*). Both arrhythmias include slowing of sinus rate (longer P–P intervals) and of AV conduction (a longer P–R interval before the pause), indicative of simultaneous inhibition of the sinoatrial and AV nodes by the vagus nerve. P, atrial depolarizations; R, ventricular depolarizations. (*C*) HRV in WT (squares) and homozygous *Akap10*-mutant (circles) littermates, as measured by the root of the mean of squared successive differences in normal R–R intervals (RMSSD). A higher RMSSD indicates more beat-to-beat variability. (*D*) Kaplan–Meier analysis of survival in WT and mutant littermates. Differences between the three groups were tested by using Wilcoxon ($P < 0.01$) and log-rank statistical tests ($P < 0.02$). All deaths were due to natural causes, but daily monitoring of the mice by our veterinary staff did not identify any evidence of illness or distress before death. Death from arrhythmia is possible but could not be demonstrated, because no mice died during ECG recording.

In addition to sinus arrhythmia, the *Akap10*-mutant mice displayed two types of spontaneous cardiac pauses. First, sinus pauses with junctional escape beats (Fig. 3*A*) were 40 times more frequent in homozygous *Akap10*-mutant mice than in WT littermates (4/h vs. 0.1/h). Second, atrioventricular (AV) heart block was 15 times more frequent in mutants (3 vs. 0.2 nonconducted P waves per hour) (Fig. 3*B*). Both types of pauses were typically preceded by changes characteristic of vagus nerve activity: sinus slowing (prolonged P–P interval) and first-degree AV block (prolonged P–R interval) (Fig. 3 *A* and *B*). The presence in mutant mice of exaggerated sinus arrhythmia, sinus pauses, and AV heart block indicates that the *Akap10* mutation causes excessive vagus nerve sensitivity.

***Akap10*-Mutant Mice Die in Adulthood.** To determine whether *Akap10* is important for survival, we examined the lifespan of *Akap10*-mutant mice. The *Akap10* mutation shortened mouse lifespan in a dose-dependent manner (Fig. 3*D*). Approximately 50% of homozygous and 25% of heterozygous mice died in the first year of life. None of their WT littermates died during this time. The lethal effects of the *Akap10* mutation occurred only in adults: mutant pups were born at the expected Mendelian frequency, and the youngest death occurred at the age of 4 months. The cause of death remains unclear. The mice displayed no evidence of overt illness before death. Mutant mice had normal blood chemistry and hematology and no signs of organ histopathology (SI Table 4). The lack of pathologic findings along with the abnormal ECGs is consistent with death from arrhythmia. Interestingly, the mortality phenotype is markedly affected by the genetic background of the mice. The original studies (Fig. 3*C*) were performed on a 129/ola mouse background. We later repeated this experiment on a FVBN mouse background and found no apparent early death for the AKAP10 mutant mice. This result suggested a stain-dependent effect that may merit further genetic analysis. The AKAP10 mutant mice back-crossed into the FVBN background will be deposited into a public repository (www.mmrrc.org).

Table 3. Effects of *AKAP10* genotype on HR and HR variability in humans

95% confidence interval	V/V vs. I carriers	I/I vs. V carriers
Average HR >75		
Odds ratio	1.02	0.40
95% confidence interval	0.38–2.74	0.17–0.94
P	0.97	0.03
Minimum HR		
Estimated effect	+3.2 bpm	0.84 bpm
Standard error	1.79	1.56
P	0.08	0.59
HR variability (SDNN)		
Estimated effect	−19.66 ms	−0.34 ms
Standard error	9.25	8.09
P	0.04	0.97

***I646V* SNP Alters HR and HRV in Humans.** We suspected that genetic variation of Akap10 might affect vagus nerve sensitivity in humans. The human I646V polymorphism changes the affinity of Akap10 for R1 regulatory subunits of PKA (11). Because the mouse *Akap10* mutation that lacks PKA binding increased vagus nerve sensitivity, we predicted that the minor human allele, *646V*, which has a high binding affinity for PKA, would decrease vagus nerve sensitivity.

To test this possibility, we genotyped 122 participants in the Heart and Soul Study (27, 28) who had 24-h continuous ECG recording. As predicted, *646V* was associated with markers of low vagus nerve sensitivity: fast HR and low HRV. Carriers of *646V* were more likely to have a mean HR (over 24 h) >75 min^{-1} (59% vs. 35%, $P \leq 0.03$), which is an independent risk factor for sudden cardiac death in the general population (29). The effect of *646V* on HR was particularly apparent when vagus nerve activity was high and HR was slow: the minimum HR (over the 24-h recording period) in *646V* homozygotes averaged 55.0 ± 1.9 min^{-1} as compared with 50.7 ± 0.7 min^{-1} in others ($P \leq 0.02$). The *646V* homozygotes also had lower HRV than others, as measured by the standard deviation of normal cardiac cycle lengths (SDNN): 111 ± 6.2 vs. 129 ± 4.2 ms, $P \leq 0.04$. Low SDNN is an independent predictor of cardiac mortality and sudden death in patients with cardiac disease (2). Multivariate analysis suggested that the effects of the *AKAP10* alleles were largely independent of race, gender, age, and other cardiac risk factors (Table 3 and SI Fig. 6). Although the mouse mutation and human AKAP10 SNP are structurally very

different, each result suggests that AKAP10 regulates pacemaker function and vagus nerve sensitivity.

Discussion

Our study suggests that *AKAP10* regulates heart rhythm by modulating the sensitivity of cardiac cells to cholinergic vagus nerve inputs. The molecular mechanism of this effect is unknown at this time, yet findings in mESC-derived embryoid bodies (EBs), mice, and humans all suggest the same conclusion. Mutation of mouse *Akap10* increased the sensitivity of cultured cardiac cells to cholinergic signals, and this result was reproduced in living mice. We also noted an increased beat-to-beat variability in *Akap10*-trap EBs that reproduced in living mice with increased HRV. This finding could suggest that beat-to-beat variability is intrinsic to individual cardiac myocytes in culture, or it could reflect the complex paracrine signaling among cells in an EB. The biology of cardiac myocytes in EBs is still just beginning to be explored, but early findings suggest that adrenergic and cholinergic systems develop within EBs (30). Although we are just beginning to understand this system, our results suggest that studies in hESC-derived myocytes will be relevant to cardiovascular genetics and pharmacology.

Our findings in humans suggest that a role of *AKAP10* in heart rhythm has been conserved in humans and mice. We found that genetic variation in human *AKAP10* associated with vagus nerve sensitivity as measured by HR and HRV. Others have reported that human *AKAP10* variants also affect cardiac AV conduction (11), analogous to our findings in the mutant mice. However, great caution must be taken when comparing cardiovascular findings in mice with those in humans because there are many differences, including the fact that HR is nearly 10 times faster in mice than in humans. Also, it would be impossible to adequately evaluate the *646V* SNP in mice because mice are WT for this allele. Fortunately, recent advances in human ESC culture may soon make genetic manipulations common with mouse ESCs in human ESC-derived myocytes (30). Then, for the first time, we will have a genetically tractable system to directly examine human cardiac myocytes. Our initial studies in mESCs provide encouraging preliminary data for the eventual transition to human ESC systems.

Cholinergic signals from the vagus nerve seem to reduce susceptibility to ventricular arrhythmias and sudden cardiac death (2, 29, 31–35). A role for *646V* in sudden cardiac death risk could explain why the incidence of this allele is disproportionately low among healthy older people. A large-scale genetic study of aging found that 646V was the most significantly underrepresented SNP in healthy people over age 60, of 6,500 SNPs tested (11). Sudden cardiac death kills 400,000–460,000 Americans every year, accounting for 15% of all deaths (36). Any effect of *646V* on sudden cardiac death risk would be small compared with the effects of genetic mutations that cause familial arrhythmias, but the population impact could be large. An estimated 14–17% of Americans (≈43 million) are homozygous for *646V* (ref. 11 and W. Tingley, J. Zaroff, and M. Whooley, unpublished data from the Heart and Soul Study). Our own data suggest that there could be a link between *646V* and key risk factors for sudden cardiac death (low HRV and higher basal heart rate), but we have not established a causal relationship, and the *646V* could have other physiological effects that we have not examined (3, 37). Future studies will be needed to directly test the association between sudden cardiac death and *646V*. The identification of genetic risk factors for sudden cardiac death should lead to improvements in risk stratification, which is critical for effective prevention. Genetic screens in stem cell-derived myocytes may help identify additional genes that contribute to cardiac arrhythmia and heart disease.

Materials and Methods

ES Cell Culture and Differentiation. Pluripotent mESCs (129/OlaHsd strain, subline E14Tg2A.4) were maintained without feeder cells in the presence of leukemia inhibitory factor (38) and differentiated into cardiac myocytes as described (10, 39). Briefly, 20-μl droplets of differentiation medium [ES cell medium (38) without leukemia inhibitory factor and with 20% FBS] containing 450–550 mESCs were suspended upside-down for 2 d, causing the cells to aggregate into EBs. EBs were maintained in suspension cultures for 5 d and then plated onto gelatin-coated, 24-well tissue-culture plates (one EB per well). The medium was replaced every 2–3 d. Beginning on day 8 of differentiation, clusters of myocytes within the EBs contracted spontaneously (SI Movie 1).

Gene-Trap Mutagenesis of Akap10. Details of the *Akap10*-mutant cell line (RRC139) and protocols for gene-trap mutagenesis (38) in mESCs can be found at http://baygenomics.ucsf.edu/protocols/index.html. The location of the gene-trap vector (pGT1lxf) insertion in the ES cell genome was determined by genomic PCR and DNA sequencing. The mutagenic insertion occurred in only one *Akap10* allele and was not associated with the deletion of any flanking genomic sequences as determined by PCR analysis of the junction sites. Truncation of *Akap10*-mutant mRNA after exon 12 and fusion with the gene-trap vector sequences were confirmed by 5′ rapid amplification of cDNA ends and sequencing as described (38). Akap10 protein sequences (Fig. 1*E* and SI Fig. 4) were from Ensembl [human, chimp, dog, rabbit, cow, opossum, mouse, rat, chicken, frog t. (*Xenopus tropicalis*)], zebrafish, pufferfish (tetraodon and fugo), and NCBI [monkey, pig, frog l. (*Xenopus laevis*)].

Contraction Rate Analysis of ES Cell-Derived Myocytes. After 12–16 d of differentiation, groups of spontaneously contracting myocytes were filmed with phase microscopy (Zeiss, Thornwood, NY) and a video camera (10 frames per second; Cohu, San Diego, CA) linked to digital imaging software (OpenLab, Cambridge, U.K.). We programmed the software to quantify changes in the amount of transmitted light as the cells contracted. Each contraction was identified with a custom algorithm and confirmed manually. *Akap10*-mutant and WT EBs were maintained in neighboring wells of 24-well tissue-culture plates and treated identically. Experiments were performed at 20°C in 138 mM NaCl, 8 mM Na_2HPO_4, 2.7 mM KCl, 1.47 mM K_2PO_4, 0.9 mM $CaCl_2$, and 0.5 mM $MgCl_2$ (pH 7.1) (Dulbecco's PBS; Invitrogen, Carlsbad, CA). Carbachol and dobutamine (Tocris, Ellisville, MO) were prepared in the same solution and added to the EBs as a 1:2 dilution. Average contraction rates (Table 1) were determined over the 70 s immediately before (baseline) and 15–85 s after addition of the drug. For the carbachol experiments, to minimize any possible confounding effects of different baseline rates between WT and mutant cells, cells with similar baseline rates were selected for drug treatment and analysis. Addition of vehicle did not affect the contraction rate.

Mouse HR and ECG Recordings. ECG telemeters (TA10EA-F20; Data Sciences International, St. Paul, MN) were implanted into adult male and female mice (>10 weeks old), according to the manufacturer's protocols. Data were collected from conscious animals freely moving in their home cages, beginning at least 1 week after surgery to allow full recovery from anesthesia. Methacholine (acetyl-β-methylcholine, 2 mg/kg; Sigma, St. Louis, MO) or phenylephrine (2 mg/kg; Sigma) was injected into the i.p. cavity at a volume equivalent to 1% of the animal's weight, and heart rates were recorded every 10 s continuously. Injection with normal saline carrier caused tachycardia in WT and *Akap10*-mutant mice, to the same degree, perhaps because of anxiety from the procedure. HRs in Table 1 represent the average HR over the 5 min immediately before (baseline) and 1–5 min (methacholine) or 2–12 min (phenylephrine) after injection. Baseline beat-to-beat HRV was quantified by calculating the square root of the mean of the squared differences between adjacent normal R–R intervals (35), by using at least 5,000 adjacent normal R–R intervals from continuous ECG recordings in untreated animals. Segments of the ECG recordings

that contained artifacts were identified manually and discarded. R waves were identified with Data Sciences International software and confirmed manually. Arrhythmias were quantified by manual inspection of 60 h of ECG recordings over multiple times of the day from conscious mice (four homozygous *Akap10*-mutant mice and four WT littermates). For the purpose of quantification, we defined a sinus pause with junctional escape as a P–P interval more than twice the prior PP and containing a narrow-complex QRS in the second half of the interval. A nonconducted P wave was a nonpremature P wave followed by another nonpremature P wave without an intervening QRS complex.

Mouse Survival and Pathology Screening. Survival of *Akap10*-mutant homozygous, heterozygous, and WT littermates (housed together) was analyzed with the Kaplan–Meier method. Mortality rates were similar in males and females. Three mice (all heterozygous) developed unrelated eye and skin lesions and were excluded. Histopathologic, serum chemistry, and hematologic analyses of three homozygous and three WT littermates (20–28 wks of age) were performed by Stephen M. Griffey of the Comparative Pathology Laboratory, School of Veterinary Medicine, University of California, Davis. No important abnormalities were detected in 48 tissues examined: adrenal glands, aorta, bone marrow, brown fat, cecum, cerebrum, cerebellum, colon, rectum, costochondral junction, diaphragm, dorsal skin, esophagus, eye, lacrimal gland, femur, hardarian gland, heart, inner ear, kidneys, liver, gall bladder, lung, trachea, mesenteric lymph node, nasal cavity, pancreas, peripheral nerve, pituitary gland, quadriceps muscle, reproductive tract (accessory sex glands, urethra, testes), salivary glands (sublingual, parotid, mandibular), small intestine, spinal cord, spleen, sternum, stomach, submandibular lymph node, tail, teeth, thymus, thyroid gland, parathyroid glands, tongue, and urinary bladder.

Human HR and HRV Analysis. Data were obtained from patients with stable coronary heart disease enrolled in the Heart and Soul Study (27, 28); 682 participants underwent three-channel, 24-h ambulatory ECG monitoring, standardized exercise treadmill testing, and AKAP10 I646V genotyping. For this analysis, we excluded 54 participants who were not in sinus rhythm and 506 participants who were taking antihypertensive medications that affect HR or HRV, leaving 122 participants (mean age, 64 yr; 22% women). This cohort included 46 (38%) *646I* homozygotes, 26 (21%) *646V* homozygotes, and 50 (41%) heterozygotes. We measured HRV indices as described (28). Software (GE Healthcare, Waukesha, WI) was used to identify all normal (NN) cardiac cycles (sequential QRS complexes with normal morphologic characteristics and a cycle duration within 20% of the preceding cycle) and compute time-domain HRV variables, including SDNN. All processed data were confirmed manually and edited where necessary by a blinded reviewer. Age, gender, ethnicity, smoking status, medical comorbidities, cardiac symptoms, and physical activity were determined by questionnaire; body mass index was measured, and exercise capacity was determined by standardized exercise treadmill testing. All participants provided written informed consent after the nature and possible consequences of the studies were explained, and the appropriate institutional review boards approved the protocol.

Human Genotyping. The template-directed dye-terminator incorporation assay with fluorescence polarization detection (FP-TDI) (14) was used to determine *AKAP10 I646V* (rs203462) genotype in 986 participants of the Heart and Soul Study (27, 28) who consented to genotyping.

Generation of Akap10-Mutant Mice, Akap10 Immunoblots, FP-TDI Conditions, and Statistics. See *SI Methods* for generation of Akap10-mutant mice, Akap10 immunoblots, and statistics.

We thank Drs. Jeffrey Olgin, Paul Simpson, William Grossman, Robert Mahley, Deepak Srivastava, Lily Jan, Susan Taylor, Lora Burns-Hamuro, Charles Cantor, Andreas Braun, Neil Risch, and Shaun Coughlin and members of the B.R.C. laboratory for valuable discussions; Stephen Ordway and Gary Howard for editorial assistance; Kristen Lum and Annie Poon for technical assistance; and Mary Weglarz for assistance with manuscript preparation and submission. This work was supported by the American Heart Association (0275033N), the J. David Gladstone Institutes, a Grove Stem Cell Challenge grant, National Heart, Lung, and Blood Institute Grants HL66621and HL60664, National Center for Research Resources Grant RR18928, and the Department of Veterans Affairs.

1. Levine H (1997) *J Am Coll Cardiol* 30:1104–1106.
2. Barron H, Lesh M (1996) *J Am Coll Cardiol* 27:1053–1060.
3. Beene D, Scott J (2007) *Curr Opin Cell Biol* 19:192–198.
4. Lynch M, Baillie G, Mohamed A, Li X, Maisonneuve C, Klussmann E, van Heeke G, Houslay M (2005) *J Biol Chem* 280:33178–33189.
5. Gardner L, Tavalin S, Goehring A, Scott J, Bahouth S (2006) *J Biol Chem* 281:33537–33553.
6. McConnachie G, Langeberg L, Scott J (2006) *Trends Mol Med* 12:317–323.
7. Michel JC, Scott J (2002) *Annu Rev Pharmacol Toxicol* 42:235–257.
8. Liggett SB (2003) *Assay Drug Dev Technol* 1:317–326.
9. Sowell M, Ye C, Ricupero D, Hansen S, Quinn S, Vassilev P, Mortensen R (1997) *Proc Natl Acad Sci USA* 94:7921–7926.
10. Boheler K, Czyz J, Tweedie D, Yang H, Anisimov S, Wobus A (2002) *Circ Res* 91:189–201.
11. Kammerer S, Burns-Hamuro L, Ma Y, Hamon S, Canaves J, Shi M, Nelson M, Sing C, Cantor C, Taylor S, Braun A (2003) *Proc Natl Acad Sci USA* 100:4066–4071.
12. Burns-Hamuro L, Ma SY, Kammerer S, Reineke, Self C, Cook C, Olson G, Cantor C, Braun A, Taylor S (2003) *Proc Natl Acad Sci USA* 100:4072–4077.
13. Burns-Hamuro L, Barraclough D, Taylor S (2004) *Methods Enzymol* 390:354–374.
14. Hsu T, Chen X, Duan S, Miller R, Kwok P (2001) *BioTechniques* 31:560, 562, 564–8, passim.
15. De-Zolt S, Schnutgen F, Seisenberger C, Hansen J, Hollatz M, Floss T, Ruiz P, Wurst W, von Melchner H (2006) *Nucleic Acids Res* 34:e25.
16. Stryke D, Kawamoto M, Huang C, Johns S, King L, Harper C, Meng E, Lee R, Yee A, L'Italien L, *et al.* (2003) *Nucleic Acids Res* 31:278–281.
17. Wickman K, Nemec J, Gendler S, Clapham D (1998) *Neuron* 20:103–114.
18. Hamuro Y, Burns L, Canaves J, Hoffman R, Taylor S, Woods V (2002) *J Mol Biol* 321:703–714.
19. Doupnik C, Davidson N, Lester H, Kofuji P (1997) *Proc Natl Acad Sci USA* 94:10461–10466.
20. Chuang H, Yu M, Jan Y, Jan L (1998) *Proc Natl Acad Sci USA* 95:11727–11732.
21. Bunemann M, Hosey M (1998) *J Biol Chem* 273:31186–31190.
22. Saitoh O, Kubo Y, Odagiri M, M Ichikawa, Yamagata K, Sekine T (1999) *J Biol Chem* 274:9899–9904.
23. Herlitze S, Ruppersberg J, Mark M (1999) *J Physiol (London)* 517(Pt 2):341–352.
24. Kurachi Y, Ishii M (2004) *J Physiol (London)* 554:285–294.
25. Benians A, Nobles M, Hosny S, Tinker A (2005) *J Biol Chem* 280:13383–13394.
26. Spiegel A, Weinstein L (2004) *Annu Rev Med* 55:27–39.
27. Ruo B, Rumsfeld J, Hlatky M, Liu H, Browner W, Whooley M (2003) *J Am Med Assoc* 290:215–221.
28. Gehi A, Ix J, Shlipak M, Pipkin S, Whooley M (2005) *Am J Cardiol* 95:1474–1477.
29. Jouven X, Empana J, Schwartz P, Desnos M, Courbon D, Ducimetiere P (2005) *N Engl J Med* 352:1951–1958.
30. Reppel M, Boettinger C, Hescheler J (2004) *Cell Physiol Biochem* 14:187–196.
31. La Rovere MT, Pinna GD, Hohnloser SH, Marcus FI, Mortara A, Nohara R, Bigger JT, Jr, Camm AJ, Schwartz PJ (2001) *Circulation* 103:2072–2077.
32. Stein P, Kleiger R (1999) *Annu Rev Med* 50:249–261.
33. Villareal R, Liu B, Massumi A (2002) *Curr Atheroscler Rep* 4:120–127.
34. Schwartz PJ, Rovere MT, Vanoli E (1992) *Circulation* 85:I77–I91.
35. Task Force of the European Society of Cardiology (1996) *Circulation* 93:1043–1065.
36. Zheng Z, Croft J, Giles W, Mensah G (2001) *Circulation* 104:2158–2163.
37. Wirtenberger M, Schmutzhard J, Hemminki K, Meindl A, Sutter C, Schmutzler R, Wappenschmidt B, Kiechle M, Arnold N, Weber B, *et al.* (2007) *Carcinogen* 28:423–426.
38. Skarnes W (2000) *Methods Enzymol* 328:592–615.
39. Wobus A, Guan K, Yang H, Boheler K (2002) *Methods Mol Biol* 185:127–156.